Lab on a Chip

Accepted Manuscript

This is an *Accepted Manuscript*, which has been through the Royal Society of Chemistry peer review process and has been accepted for publication.

Accepted Manuscripts are published online shortly after acceptance, before technical editing, formatting and proof reading. Using this free service, authors can make their results available to the community, in citable form, before we publish the edited article. We will replace this *Accepted Manuscript* with the edited and formatted *Advance Article* as soon as it is available.

You can find more information about *Accepted Manuscripts* in the **Information for Authors**.

Please note that technical editing may introduce minor changes to the text and/or graphics, which may alter content. The journal's standard **Terms & Conditions** and the **Ethical guidelines** still apply. In no event shall the Royal Society of Chemistry be held responsible for any errors or omissions in this *Accepted Manuscript* or any consequences arising from the use of any information it contains.

Graphical Abstract

Muscle actuators are typically densely populated cells cultured in 2D sheets or 3D matrices of fibrous proteins that self-assemble into a bulk, monolithic muscle strip. We demonstrate a novel technique to construct parallel assemblies of smaller muscle strips that maximize the volume of active muscle layers, thereby augmenting contractile force generation. In tandem with multiple muscle strips, external control through the use of optogenetics can selectively recruit muscle strips for the gradation of these forces. This would not only facilitate larger-scale muscle actuators by bypassing the need for an in vitro vasculature, but also potentially create new functionalities.
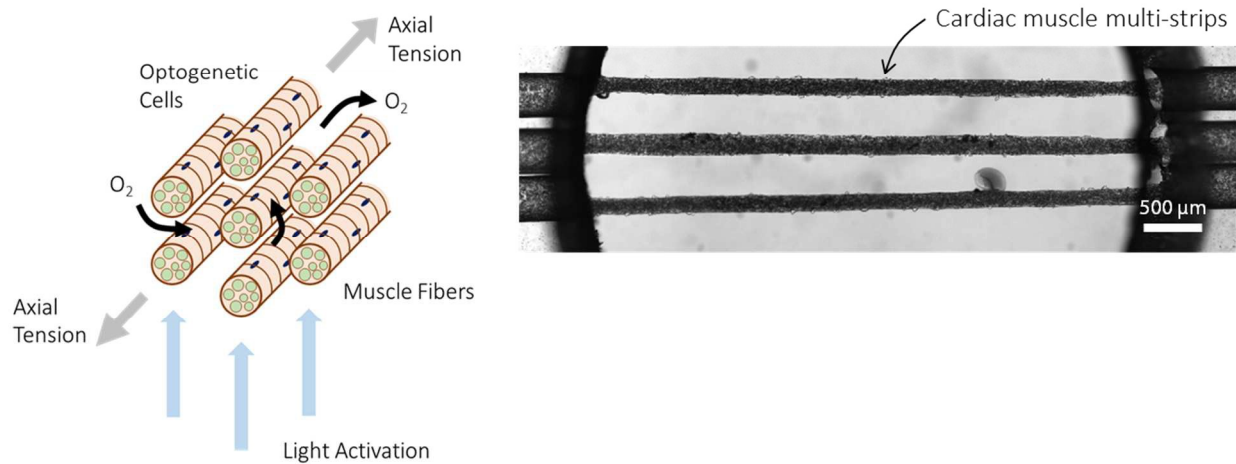
Fabrication and Characterization of Optogenetic, Multi-Strip Cardiac Muscles

Vincent Chan[a*], Devin Neal[a], Sebastien Uzel[a], Hyeonyu Kim[a], Rashid Bashir[b] and H. Harry Asada[a]

[a] Department of Mechanical Engineering, Massachusetts Institute of Technology, Cambridge, MA USA 02139
[b] Department of Bioengineering, Micro and Nanotechnology Laboratory, University of Illinois at Urbana-Champaign, Urbana, IL USA 61801
[*] To whom correspondence should be addressed. E-mail: chanv@mit.edu

Abstract

Cardiac tissue engineering aims to recreate functional tissue constructs similar to the structure and function of the native myocardium. To date, in vitro tissue constructs lack the architectural complexity of a vascular network and the precise motor unit control of muscle fibers. Here, we present a method to construct engineered multi-strip cardiac muscle that simulates the bundle-like architecture of the native myocardium. Densely packed primary myocytes and cardiac fibroblasts were co-cultured with optogenetic, non-excitable cells. The resulting 3D syncytium triggered contraction upon localized blue light illumination to selectively activate and pace the multi-strip cardiac muscles, similar to the activity of pacemaker cells. Acting on a single load, we demonstrated graded force production through light-modulated multi-strip recruitment. These results demonstrate an in vitro platform of optogenetic, multi-strip cardiac muscles that can be used in a wide variety of applications, such as drug discovery, tissue engineering, and bio-hybrid robotic systems.

Introduction

Structurally, the heart is an extremely complex organ, and its function is vital to survival. It is composed of tightly packed myocytes and fibroblasts that surround dense vasculature and is supported by collagen-based extracellular matrix (ECM) proteins [1]. The myocytes are the contractile cells of the heart that form a 3D syncytium through specialized intracellular junctions. These junctions enable the propagation of electrical signals to produce mechanical contractions that are used to support heart function and blood flow [2].

Cardiac tissue engineering aims to recreate functional tissue constructs similar to the structure and function of the native myocardium. Generally, there are two methods for constructing engineered cardiac tissue. Firstly, the 2D "cell sheet engineering" method is a technique for harvesting monolayers of cardiac myocytes to preserve their cell-cell junctions and cell surface proteins [3, 4]. The core principle is to culture cells on a thermoresponsive polymer (*i.e.* PNIPAAm) that can reversibly change between hydrophobic (> 32 °C) and hydrophilic (< 32 °C) states. The cell sheet detaches and can be harvested at temperatures below 32 °C, known as its lower critical solution temperature (LCST). Secondly, the 3D "engineered heart tissue" method is a technique that embeds cells in 3D collagen gels cast around either Velcro covered glass tubes [5] or circular Teflon molds [6]. The addition of an extracellular matrix milieu secreted by Engelbreth-Holm-Swarm mouse sarcoma cells (*e.g.* Matrigel) to the initial reconstitution mixture is necessary for exhibiting differentiation, growth, and tissue formation [6].

The advantage of 2D cell sheet engineering is the ability to attach one cell sheet on top of another cell sheet [7]. This allows 3D tissues to be formed by simply layering them on top of

1

each other. High-throughput fabrication of cell sheets has also been demonstrated using a custom-built automated cell sheet stacking apparatus, which uses a plunger-like manipulator coated with gelatin to pick up the sheets and stack them on top of each other [8]. Cell sheet technology has been well-studied, and clinical trials in the myocardium are underway [9]. However, 2D cell sheets do not capture the 3D architectural complexity of cardiac tissues in vivo. Myocytes in the native myocardium are highly aligned by axially-applied mechanical stress, and assemble into 3D spatially-organized bundles [10]. In addition, myocytes establish specialized intracellular connections with neighboring cells, such as gap junctions and desmosomes [2]. While stacking cell sheets can create pseudo-3D constructs, they are limited by ischemic conditions originating from a lack of perfusion.

Alternatively, the advantage of the 3D engineered heart tissue mold is that it allows for minimal handling and easy transfer. The circular molds lead to better tissue formation than the original lattice design because the circular geometry causes a homogenous force distribution throughout the tissue. Chronic cyclic stretch of engineered heart tissues improves contractile force and induces better cardiac tissue development [11]. Engineered heart tissues have been implanted in infarct rat hearts and shown to improve their function [12]. However, 3D engineered heart tissues also suffer from diffusion-based processes and result in low volumetric cell density in its central regions [5, 6]. In the native myocardium, bundles form within 100 μm of supporting blood vessels for a continuous supply of oxygen and nutrients. Moreover, unlike cardiac tissue constructs, the rhythmic contractions of spatially distributed tissue in the native myocardium are controlled by a subpopulation (< 1%) of myocytes called pacemaker cells in the right atrium [13]. Propagation of action potentials occurs through specialized myocytes in the sinoatrial node and Purkinje fibers. Additionally, sympathetic and parasympathetic nerve fibers constantly modify the rate of depolarization in the myocardium [14]. All of these factors are critical requirements for overall cardiac function and maturation in vitro.

Here, we present a method [15] for constructing engineered multi-strip cardiac muscle that simulates the bundle-like assembly of the native myocardium. Driven by cell-mediated compaction, each strip was formed between two anchor points to generate uniform axial tension promoting cell alignment and maturation. The composition of the muscle strips was a collection of densely packed primary myocytes and fibroblasts interspersed with non-excitable cells that expressed channelrhodopsin-2 [16, 17], an exogenous protein that functions as a light-gated ion channel. The resulting 3D syncytium of electrically-coupled, heterogenic cells was triggered to contract upon blue light illumination through electric wave propagation initiated by the non-excitable cells. By constraining size and position of blue light illumination, we demonstrated selectivity over activation and rate of contraction of the muscle multi-strips, similar to the activity of pacemaker cells. With these combined capabilities to scale the number of cardiac muscle multi-strips in a single device and to control their contractions with high spatiotemporal resolution, we further demonstrated graded force production through multi-strip recruitment. The end product is an in vitro platform of multi-strip cardiac muscle that can be used in a wide variety of applications, such as drug discovery, tissue engineering, and bio-hybrid robotic systems.

Results

Design of optogenetic, multi-strip cardiac muscles

We created an in vitro platform to fabricate optogenetic, multi-strip muscles that closely mimics the fiber clustering design of skeletal muscle (Figure 1A). While we reported successful formation of cardiac fibers with this design, it can also be extended for clustering skeletal fibers [15, 18]. The platform was designed to produce multi-strip muscles with: (1) a truly 3D form, (2) highly aligned cells and fibrin structure generated through axial stress, (3) a composition of myocytes and fibroblasts interspersed with non-excitable cells that expressed channelrhodopsin-2, and (4) a parallel arrangement of muscle strips that were spaced evenly apart from one another so that the bundles were well-perfused.

Structurally, myocytes in the native myocardium are organized into densely packed bundles that wrap around vasculature. Up to now, in vitro tissue constructs lack a proper vascular network and display poor perfusion, preventing them from being scaled up without causing a necrotic core [19]. In contrast, individual cardiac muscle strips in our multi-strip arrays were not tightly arranged, but were spaced evenly apart, to promote uniform perfusion of oxygen and nutrients (**Figure 1B**). This enabled us to easily scale the number of cardiac muscle strips in our multi-strip arrays beyond the overall size that would be permissible in monolithic bulk cardiac muscles without vasculature.

Functionally, optogenetic, multi-strip cardiac muscles were designed to imitate the control of muscle fibers in the human body. Sympathetic and parasympathetic nerve fibers constantly modify the rate of depolarization in the myocardium [14]. Motor neurons recruit one or up to a thousand muscle fibers, and each one of these groups is known as a motor unit [20]. While we did not attempt to recreate these physiological structure-function relationships, our in vitro construct does capture the function through light modulation with optogenetic technology. By spatially localizing the light, we were able to selectively recruit any combination of muscle strips similar to in vivo muscle fiber control (**Figure 1C**).

Fabrication and formation of multi-strip cardiac muscles

We modified our previously reported Sacrificial Outer Molding (SOM) technique [15] to accommodate for the formation of multi-strip cardiac muscles using a 6-step process (**Figure 1D**). Multiple pins were utilized within the same platform to produce clusters of muscle strips organized in parallel arrays. The PDMS device was designed to have three wells with steel pins inserted into the through holes of the two outer wells (**Figure 1E**). The outcome of the SOM technique was an array of elongated cardiac muscle strips that formed within the two outer wells (**Figure 1F and 1G**). The middle well served as a medium reservoir for the perfusion of muscle strips in both wells. The outer wells were 5 mm in diameter. The well diameter correlated to the length of the cardiac muscle strips, provided that the through holes passed through the center of the outer wells. The steel pins were 356 μm (0.014") in diameter and spaced roughly 500 μm apart. The pin diameter correlated to the initial diameter of the cardiac muscle strips.

The morphology of cells within individual tissue constructs was monitored using time-lapse brightfield microscopy (**Figure 2A**). Images showed high volumetric density of cells following tissue formation. Immediately after seeding the mixture of cells and matrix into the through holes, the diameter of the cardiac muscle strips contracted from 356 μm to 324 ± 10 μm. The final diameter of the cardiac muscle strips was dependent on a variety of factors influencing cell-mediated gel compaction, including cell type and concentration, matrix composition, and soluble factors. For our parameters (as described in the *Materials and Methods*), an initial pin diameter of 356 μm yielded a cardiac muscle strip diameter that stabilized around 138 ± 62 μm, or more than 60 % gel compaction (**Figure 2B**). Similar to previous reports [21], the majority of cell-mediated gel compaction (over 50 %) transpired within 24 hr of culture. The temporal response was comparable for bulk changes in muscle strip diameter regardless of the initial pin diameter (**Figure S1**).

Despite stabilization of its diameter following cell-mediated gel compaction, the cardiac muscle strips began to degrade rapidly after 5 days in culture. This was evident by the increasingly large standard deviations in strip diameter from 5 to 7 days (**Figure 2C**). An image of the cardiac muscle strip after 7 days illustrates the non-uniform cross-section and its eventual break down (**Figure S2A**). To effectively slow the degradation process, we supplemented the culture medium with ε-aminocaproic acid (EACA), a protease inhibitor. Cardiac muscle strips with EACA (2 mg ml^{-1}) at low concentrations were structurally stable and functionally contractile for a longer lifetime than without EACA (**Figure S2B**). At high concentrations (10 mg ml^{-1}), however, EACA was found to be toxic to the cardiac myocytes.

Characterization of cells within individual muscle strips

Viability of muscle tissue constructs were evaluated after 6 hr with a fluorescent-based assay using calcein-AM for live cells and ethidium homodimer-1 for dead cells (**Figure 2D**). While there was a significant proportion of dead cells (~ 30%) in the construct, this is not uncommon due to the harsh isolation conditions associated with enzymatic digestion. The surviving myocytes required at least 24 hr of recovery time after isolation. After 48 hr in culture, the cell density increased significantly as indicated by the change in opacity. Insets of the time-lapse images revealed cells that were initially spherical, but became aligned later due to the interplay of cell traction, fibrillary network deformation, fibril alignment, and cell contact guidance.

Between 24 - 48 hr, there was clear evidence of single cell contraction (**Movie S1**). As the cells began to extend and retract their thin protrusions, they create specialized intercellular connections between them through gap junctions, which directly connects the cytoplasm of two cells and allows various molecules and ions to pass freely between cells. Gap junctions are particularly important in cardiac muscle as the signal to contract is passed efficiently, allowing the heart muscle cells to contract in tandem. Single cell and subsequent regional spontaneous contractions of the cardiac muscle strips are evident after 76 hr (**Movie S2**). By 120 hr, most of the cells had extended and aligned along the longitudinal axis of the muscle strip. The cells were mostly connected in one large 3D syncytium, which is synchronized electrically in an action potential (**Movie S3**). Myocytes and fibroblasts incubated with fluorescently tagged with

antibodies against mouse sarcomeric α-actinin, filamentous actin, and counterstained with DAPI (nuclei) (**Figure 2E**).

Optical stimulation of cardiac muscle strips

The concept of the "tandem cell unit" strategy for optogenetics was first developed by Jia *et al*. [17]. Many cells have intercellular bridges including gap junctions with their neighbors that enable them to communicate directly. Gap junctions are important in a number of physiological processes, particularly in the coordinated depolarization of cardiac muscle. The tandem cell unit strategy exploits the use of gap junctions to control cardiac muscle through optogenetics by transfecting a cell line that has the same gap junctions as primary cardiac myocytes. In this case, primary cardiac myocytes are abundant with connexin-43 (Cx43) gap junctions. In our experiments, we used the human embryonic kidney 293T (HEK293T) cell line because (1) it expresses Cx43 gap junctions and (2) it uptakes plasmid DNA with high efficiency. Primary cardiac myocytes co-cultured with HEK293T cells form a syncytium that can be controlled through optical depolarization of HEK293T cells and electrical propagation through their Cx43 gap junctions (**Figure 3A**).

The DNA plasmid enclosing channelrhodopsin-2 (ChR2) was successfully transfected into the HEK293T cell line using Lipofectamine 2000. To select for cells with high expression of ChR2, we sorted the cells using the green fluorescent protein (GFP) tags attached to the ChR2 ion channels followed by ultra-low plating (< 10 cells) of ChR2-HEK293T in a 96-well plate. A uniform colony of ChR2-HEK293T cell was selected and expanded out (**Figure 3B**). This colony was co-cultured with primary cardiac myocytes at different ratios. One thing to consider is that HEK293T cells are highly proliferative, while myocytes are no longer or limited in their proliferation. We found an optimal ratio of 1:20 HEK293T cells-to-myocytes.

Whole cell patch clamping was used to verify optical depolarization of HEK-ChR2 cells. A single pulse of blue light (1 second) resulted in the depolarization of the patched HEK-ChR2 cell (**Figure 3C**). The cells were also stimulated at 5 Hz, 20 Hz, and 30 Hz frequencies (**Figure 3D, 3E, and 3F**). Between 20 – 30 Hz, ChR2-triggered depolarizations in the HEK cells started to overlap the refractory periods of preceding depolarizations. We also verified propagation of the depolarized ChR2-HEK293T into a primary cardiac myocyte (**Figure S3**). Schematic drawing for optical activation of cardiac muscle tissue constructs (**Figure 3G**). Brightfield microscopy of myocytes and HEK-ChR2 cells at 20:1 ratio in cardiac muscle tissue construct (**Figure 3H**). Fluorescent microscopy of HEK-ChR2 tagged with GFP-fluorescent reporter in cardiac muscle tissue construct (**Figure 3I**).

Selective recruitment of cardiac muscle multi-strips

A proof-of-concept experiment was conducted to demonstrate selective activation of multi-strip cardiac muscle using confined illumination. Three muscle strips located in close proximity to each other (≤ 1 mm) were arranged horizontally in a single device. Copper probes were used to pull their respective muscle strips a known distance before pulsing with blue light (**Figure 4A**). With only three muscle strips, eight different combinations could be generated to selectively recruit muscle strips. Here, we showed four of them (**Movie S4**): (i) bottom, (ii)

middle, (iii) bottom-middle, and (iv) bottom-middle-top (all). This was achieved by adjusting the region of exposure, such as the size and position of blue light (**Figure 4B**). The displacement of each copper probe was then tracked to measure contractility of each muscle strip.

Three observations could be made from this experiment. Firstly, contractions were limited to muscle strips exposed to blue light (**Figure 4C**). Only targeted muscle strips elicited a meaningful response. Generally, each muscle strip was pulsed at around 2 Hz with contraction periods lasting between 200 - 300 ms and relaxation periods lasting between 500 - 700 ms. Secondly, small perturbations in all of the non-targeted muscle strips were recorded. These perturbations were generally ≤ 5 % of the maximum strength of targeted muscle strips. One possibility is that stray light from each pulse activated myocytes in the muscle strips. Another possibility is that, since the base of all the probes were fixed at a common point, the large deflection of the targeted probe caused the non-targeted probe to vibrate. Finally, muscle fatigue was evident after multiple successions of contraction. The strength or amplitude of contraction generally dropped after each pulse (**Figure 4C**).

Gradation of contractile forces of cardiac muscle multi-strips
　　　With these combined capabilities to scale the number of cardiac muscle multi-strips in a single device and to control their contractions with high spatiotemporal resolution, we further demonstrated that force production can be graded through multi-strip recruitment. One of our key findings is a method to scale-up the force by creating multiple strips in the same device. We used three vertically-positioned muscle strips as proof-of-concept, but the number of muscle strips can be increased or decreased. The strips are kept at a minimum diameter size to reduce cell voids. With a single copper probe, we laterally stretched the muscle strips to 1.5 mm distance or ~ 15 % pre-strain (**Figure 5A and Movie S5**). The muscle strips were illuminated with blue light and the displacement of the copper probe was tracked. An animation movie of the applied tension and illuminated contraction is provided (**Movie S6**).

There were eight possible configuration states using three muscle strips. The states were grouped into four activation levels: zero, one, two, and three active or recruited muscle strips. The peak twitch forces against a single copper probe of 0.149 N/m stiffness (**Figure S4**) were 0, 2.64, 3.90, and 5.50 µN, (**Figure 5B, 5C, and 5D**) respectively. The resulting calculated stresses for a final diameter of 138 ± 62 µm were 0, 177, 261, 368 Pa, respectively. Whether one, two, or three muscle strips are recruited, the contraction period and relaxation periods remain constant at ~ 300 ms and ~ 500 ms. The peak twitch forces plotted against their activation levels showed muscle fiber recruitment-inspired control that were discrete and redundant (**Figure 5E**). A linear fit with r^2 value of 0.986 validated discretization of each muscle strip recruited.

Discussion
Compared to cell sheet engineering technology, these characteristics better capture the complex physiology of bundled cardiac muscle. It is universally accepted that 2D cultures do not produce tissues comparable to physiological systems. Specifically, 2D cultures are known to induce abnormal changes in morphology, proliferation, gene expression, and cell behavior [22].

To date, the majority of established 3D techniques employ two or more anchors, such as capped posts [23-25] or Velcro frames [19, 26, 27], around which a mixture of cells and ECM matrices (*i.e.* fibrin) compact against. While our approach utilizes a similar approach, there are a number of additional advantages that make our platform valuable.

First, the diameter and length of muscle strips can easily be tuned by cutting out wells with different biopsy punch and steel pin sizes, respectively. In particular, the diameter is crucial towards maintaining a densely packed muscle strip. Without an active vasculature, oxygen, nutrient, and waste gradients form across the muscle strip due to passive diffusion limitations. As the muscle strip increases in size, a necrotic (cell-free) core develops within the interior region [19], which affects the volume of active muscle and subsequently reduces contractile force generation.

Second, the number of muscle strips can directly be increased in a single device by adding more steel pins during the fabrication process. Rather than attempt to scale a monolithic bulk muscle strip which would result in a necrotic core, the number of muscle strips can be increased in a single device to maximize the volume of active muscle. This preserves the ratio of active muscle volume to total muscle volume that otherwise would drastically decrease in individually scaled muscle strips.

Third, optogenetic techniques with localized blue light illumination can be used for external control of multi-strip cardiac muscle. So far, external control of cardiac muscle has been limited to electric fields that activate excitable cells through propagation of action potentials. While electrical stimulation enables high temporal precision, it is either invasive by necessitating electrodes attached to or in close proximity to the muscle actuator [28], or, when used noninvasively, has poor spatial resolution.

On the other hand, optogenetics allows for user-defined spatiotemporal activation of muscle actuators by genetically programming the cells to express light-sensitive proteins [16, 25]. Since direct transfection of non-proliferative primary myocytes is tedious and the transfection efficiency is low, our approach was to co-culture a stable cell line of HEK293T that expressed channelrhodopsin-2 (ChR2) with primary myocytes [17]. These non-excitable HEK293T-ChR2 cells comprised endogenous gap junctions (connexin-43) that formed intracellular connections with myocytes. Stimulation of HEK293T-ChR2 with blue light illumination initiated action potential propagation to myocytes through these electrical couplings.

Finally, the combination of multi-strip cardiac muscle and optogenetic techniques can be used to grade contractile forces. Whereas monolithic bulk cardiac muscle generates "all-or-none" contractile forces, we have demonstrated that multi-strip cardiac muscle can be selectively recruited in a single device to accomplish increasing gradations of forces. Furthermore, as a consequence of transport limitations, the peak twitch force of monolithic bulk cardiac muscle cannot be scaled, while it is possible to scale the number of multi-strip cardiac muscles to

generate much greater twitch forces. This is similar to the physiological function of motor units, in which motor neurons can innervate a single or large subset of muscle fibers.

Taken together, we have devised a new method to form optogenetic, multi-strip cardiac muscle in a single device with our in vitro platform. The diameter and length of muscle strips can be adjusted, and the number can be scaled for selective and graded recruitment for enhanced contractile output. Moreover, this methodology can potentially be high-throughput (one-step process), and the estimated material costs are low. It also has the potential to be a general tool for forming 3D tissue with axial tension and controlled geometry.

We can extend this research to a versatile number of applications, such as "bundled" multicellular constructs (**Figure S4**). Using our sacrificial outer molding technique, we demonstrated the ability to bundle muscle strips together after their formation by removing most or all of the culture medium in the well to generate surface tension between the strips to permit physical contact. This technique can be extended to bundle multiple strips with different populations of cells. We envision co-culturing bundles of muscle and endothelial strips that are initially cultured individually to form functional muscle syncytia and vascular networks before connecting them.

One final application is the use of multiple muscle strips with free-floating bio-hybrid robotic systems (**Figure S5**) [29]. Our method would enable fast, precise, and localized stimulation of excitable tissues and their cells for neural-like control of mobile bio-robots. In tandem with multiple muscle strips in a single bio-robot, it is feasible to externally control the gradation of forces by selectively recruiting muscle strips. One day, this may lead to greater real-time control over mobile bio-robots [30-34], including the ability to toggle it on or off, specify its velocity, and even steer it, such as turning, rotating, or reversing directions. Such an alternative would not only facilitate larger-scale bio-robots by bypassing the need for an *in vitro* vasculature, but also create new functionalities of the bio-robots through external control.

Materials and Methods
Isolation and harvest of primary neonatal rat cardiac myocytes

Primary cardiac myocytes were isolated from 0 - 2 day old neonatal Sprague-Dawley rats (Charles River, Wilmington, MA 01887). All procedures were approved by the MIT Committee on Animal Care (CAC) under protocol #0913-080-16.

Whole hearts were surgically excised from neonates and homogenized by washing in ice-cold PBS. Using small scissors, ventricles were isolated and minced into ≤ 1 mm^3 tissue fragments. The minced ventricles were digested in 0.1% (w/v) purified trypsin (Worthington Biochemical, Lakewood Township, NJ 08701) in PBS with gentle agitation at 4 °C overnight. After 18 hours, warm culture medium consisting of Dulbecco's modified Eagle's medium (DMEM) supplemented with 10% (v/v) horse serum, 100 U/ml penicillin and streptomycin, and 1 mg/ml ε-aminocaproic acid (EACA) was added for 5 minutes at 37 °C to inhibit trypsin digestion. The supernatant was discarded, and 0.1% (w/v) purified type II collagenase (Worthington Biochemical, Lakewood Township, NJ 08701) was added for 45 minutes in 5 % CO_2 and 37 °C. The digested tissue was gently triturated to mechanically loosen the cells, and the suspension was filtered through a 75 μm cell strainer (BD Biosciences, San Jose, CA 95131) to remove undigested connective tissue. The suspension was removed after centrifugation at 150 × g for 5 minutes. The remaining cell pellet was re-suspended in warm culture medium and pre-plated twice for 15 minutes each to enrich the suspension for myocytes.

Generation of stable optogenetic cell line

A human embryonic kidney (HEK) 293T cell line was transfected using a DNA plasmid construct with the sequence pAAV-CAG-ChR2-GFP to generate a stable optogenetic cell line expressing the light-gated ion channel, channelrhodopsin-2 (ChR2).

HEK 293T cells were plated in a 10 cm tissue culture plate and grown in culture medium consisting of DMEM supplemented with 10% (v/v) fetal bovine serum until 90-95% confluent on the day of transfection. Antibiotics were not included in the culture medium. On the day of transfection, the culture medium was removed and replaced with 5 ml of Opti-MEM I Medium (Life Technologies, Grand Island, NY 14072). DNA-Lipofectamine complexes were prepared by mixing 3 µg of DNA plasmid and 36 µL of Lipofectamine 2000 (Life Technologies, Grand Island, NY 14072) in 3 ml of Opti-MEM I Medium without serum for 20 min at room temperature. DNA-Lipofectamine complexes were added to the plate of cells, mixed gently, and incubated overnight at 5 % CO_2 and 37 ^{o}C. The medium containing the DNA-Lipofectamine complex was replaced with 10 ml culture medium without antibiotics for at least 24 hours.

To select for stably transfected clones, cells were maintained for an extended period of time (> 2 weeks) to weed out the cells with plasmids that failed to integrate into the genome. Fluorescence-activated cell sorting (FACS, BD FACSAria II, BD Biosciences, San Jose, CA 95131) was used to remove these transiently transfected clones. Cells were plated in 96 wells at very low densities (≤ 5 cells per well) and cultured to form colonies. The desired colony was picked by carefully scraping and aspirating it with a pipette tip under a microscope. After separating the cells in a drop of trypsin solution for 5 min, they were transferred into a new well. The cells are a transfectant clone originating from a single cell with only one specific genomic integration.

Electrophysiology with whole cell patch clamp

Cultures of ChR2-expressing HEK 293T (HEK-ChR2) cells and their co-cultures with primary cardiac myocytes were carried out on gelatin-coated glass coverslips. Cells were maintained in culture medium for approximately 2 days before the patch clamp recordings. The HEK-CHR2 cells containing green fluorescent protein (GFP) tags were identified under a conventional epifluorescent microscope (Axio Observer.A1, Zeiss, Oberkochen, Germany) with a 20x objective lens (Plan-Neofluar, NA = 0.4, Zeiss, Oberkochen, Germany). The cardiac myocytes were chosen based on their light-triggered contraction mediated by the HEK-ChR2 cells.

The bath solution consisted of 115 mM NaCl, 2 mM KCl, 10 mM HEPES, 3 mM $CaCl_2$, 10 mM glucose and 1.5 mM $MgCl_2$ (pH 7.4 adjusted with NaOH). The patch pipet solution contained 140 mM K-gluconate, 5 mM KCl, 2 mM $MgCl_2$, 10 mM HEPES, 0.2 mM EGTA, 2.5 mM Na-ATP, 0.5 mM Na-GTP and 10 mM Na_2 phosphocreatine (pH 7.4 adjusted with NaOH). The resistance of the electrodes was 4 - 8 MΩ. Voltage clamp experiments were conducted with a Multiclamp 700B amplifier (Axon, Union City, CA, USA 94587) and signals were digitized at 10 kHz with an Axon Digidata 1440A interface. Data were acquired with pClamp 10 software (Axon, Union City, CA, USA 94587) and processed with the software Stimfit. The cells, held at a membrane potential of -90 mV, were subjected to pulses of blue light with an irradiance of 9 mW/mm^2 as measured by a power meter (Newport, Irvine, CA 92606) at the sample plane. Experiments consisted of either 1 s exposures followed by a resting time of 5 s, or by repeated 10 ms pulses at frequencies of 1, 5, 10, 20 and 30 Hz for 2 s. All recordings were conducted at room temperature.

Fabrication of sacrificial mold devices

A plastic master mold was 3D-printed (Dimension SST 1200es, Stratasys, Eden Prairie, MN 55344) with three vertical through-holes spaced equally apart for each sacrificial mold device. Steel pins (≥ 356 µm diameter) spanning the width of the master mold were inserted into the through-holes.

Sylgard 184 (Dow Corning Corporation, Midland, MI 48686) polydimethylsiloxane (PDMS) elastomer was mixed at a 10:1 base to curing agent ratio and degassed in a planetary centrifugal mixer (ARE-250, THINKY, Leguna Hills, CA 92653) to eliminate bubbles. The PDMS elastomer was poured into the cavity of the master mold to cover slightly more than the height of the steel pins and cured for a minimum of 4 h at 65 ^{o}C.

The cured PDMS slab was removed from the oven and cooled to room temperature. Needle-nose pliers were used to pull out the steel pins, and the PDMS slab was peeled off of the master mold. The PDMS slab was cut into multiple devices with a razor. Three well holes, 5 mm diameter and 2 mm spacing, were punched out along the central axis of the through-holes in each device using a biopsy punch (Harris Uni-Core, TedPella, Redding, CA 96049).

Steel pins were re-inserted on each side of the through-holes such that each pin spanned one of the two outer 5 mm wells to be used for cell/matrix seeding. Cellophane tape was used to clean the PDMS devices of dirt and other particles. The PDMS devices were bonded to glass coverslips using a plasma cleaner (PDC-001, Harrick Plasma, Ithaca, NY 14850) at high power setting for 1 min. Prior to cell/matrix seeding, the PDMS devices were sterilized by 70% ethanol in the wells and 30 min exposure to UV light in the biosafety cabinet. The devices were rinsed in phosphate buffer solution (PBS, Lonza, Basel, Switzerland 4002) prior to cell/matrix seeding.

Cardiac muscle multi-strip seeding

10% (w/v) gelatin from bovine skin (Sigma-Aldrich, St Louis, MO 63103) was dissolved at $\geq 37\,^{\circ}$C in culture medium, neutralized with 1% (v/v) sodium hydroxide (0.5 M in water, Sigma-Aldrich, St Louis, MO 63103), and augmented with 10% (v/v) thrombin (100 U/ml in water, Sigma-Aldrich, St Louis, MO 63103). The gelatin mixture was added to the outer wells of the PDMS device to submerge the steel pins, and it was cooled at $4\,^{\circ}$C for ≥ 45 min to solidify. The steel pins were pulled out with tweezers to leave pinholes that connected the through holes of the outer wells.

A cooled suspension of cell-laden fibrinogen (Sigma-Aldrich, St Louis, MO 63103) at 5 mg/ml in culture medium was supplemented with 10% (v/v) Matrigel (BD Biosciences, San Jose, CA 95131) and added into the pinholes of each outer well. The composition of the cells in suspension was 20:1 cardiac myocytes to HEK 293T +ChR2 ratio. The entire device assembly was incubated for 30 min at $37\,^{\circ}$C to allow the gelatin to liquefy and thrombin to diffuse into the cell/matrix mixture to induce polymerization. Culture medium was then added to all wells.

Assembly and calibration of copper probe

We previously described the force measurement device using a lateral copper probe [18]. Copper wire (Remington Industries, Johnsburg, IL 60051) either in 40 or 44 AWG size (87 or 56 µm diameter, respectively), was cut approx. 2 cm in length and mounted on a custom-made probe carrier with super glue. The carrier was fixed to a 3-axis translation stage assembled from one MT1 (X-axis) and two DT12 dovetail (Y- and Z- axes) series manual translators (Thorlabs, Newton, NJ 07860).

A laser-optical sensor (optoNCDT 1401-1, Micro-Epsilon Optronic, Ortenburg, Germany 94496) was used to measure position and displacement of the probe base. The sensor was equipped with a DC power supply (B1760A, BK Precision, Yorba Linda, CA 92887) operating at 24 V and a serial interface card (RS232, Micro-Epsilon Optronic, Ortenburg, Germany 94496) to enable operation from a standard computer. Software from the manufacturer (ILD1401 Tool v2.09, Micro-Epsilon Optronic, Ortenburg, Germany 94496) was used to measure and record output values.

Image sequences of probe tip's position and displacement were captured on the microscope stage (IX81, Olympus, Center Valley, PA 18034) by video capture software (Debut Video Capture, NCH Software, Greenwood Village CO, 80111) from a live acquisition software feed (MetaMorph, Molecular Devices, Sunnyvale, CA 94089) using a digital CCD camera (ORCA-R2C10600-10B, Hamamatsu Photonics, Bridgewater, NJ 08807).

The copper probe was calibrated by hanging known wire weights against gravity on the probe tip. The probe was mounted horizontally on the microscope stage, and tweezers were used to position the wire weights on the end of the probe tip. The optical axis of the microscope was used to measure the difference in focal planes between the loaded and unloaded tip to determine the amount of probe bending. The measurements were used to generate a load vs. displacement curves, which were then fit using linear regression.

Displacement and force measurements of contractile cardiac muscle strips

To demonstrate selective recruitment, the probes were used to track the displacement of individual contractile muscle strips. To demonstrate gradation of force, a single cantilever was used to track displacement of multiple contractile muscle strips. For all experiments, twitches were generated through optical stimulation (λ = 490 nm) at the same pre-strain conditions. Pre-strain was created by laterally displacing a cantilever probe to the point where approximately 6.8 % strain was generated along the direction of the muscle strip.

Image and video analysis

Data from the laser micrometer (measuring cantilever probe base position) and the microscope camera video (measuring cantilever tip position) was processed to generate axial tissue force and displacement. The video data provides probe tip data with the use of open source software called Tracker. Tracking the cantilever tip is robust and reliable giving sub-pixel resolution. Each individual twitch was analyzed independently. This process is shown in Supplementary Fig. S3. The tip and base data are synchronized based on a step-like input to the base position. Each twitch is segmented and combined with probe base data to determine axial strip displacement and force. Finally, each twitch is creep corrected assuming linear creep with a slope equal to the post twitch position minus the pre-twitch initial tip position divided by the twitch time. This creep correction is used to ensure that the data presented represent the force and displacements generated only by the contraction of the muscle.

Immunofluorescence

Cells and tissues were fixed with 4% paraformaldehyde in PBS, permeabilized with 0.2% Triton X-100 in PBS, incubated with antibodies against mouse sarcomeric α-actinin (Abcam, Cambridge, MA 02139), detected with Alexa Fluor 488 goat anti-mouse IgG antibodies (Life Technologies, Grand Island, NY 14072), and counterstained with DAPI (Life Technologies, Grand Island, NY 14072). Filamentous actin was visualized by incubating samples with tetramethylrhodamine-conjugated phalloidin (Life Technologies, Grand Island, NY 14072).

Acknowledgements

References

1. P. J. Hunter, A. J. Pullan AJ and B. H. Smaill, Modeling total heart function, *Annu. Rev. Biomed. Eng.*, 2003, **5**, 147-177.
2. J. M. Nerbonne and R. S. Kass, Molecular physiology of cardiac repolarization, *Physiol. Rev.*, 2005, **85**, 1205-1253.
3. T. Shimizu, M. Yamato, A. Kikuchi and T. Okano, Cell sheet engineering for myocardial tissue reconstruction, *Biomaterials*, 2003, **24**, 2309-2316.
4. Y. Yang, *et al.*, Cell sheet engineering: recreating tissues without biodegradable scaffolds, *Biomaterials*, 2005, **26**, 6415-6422.
5. T. Eschenhagen, *et al.*, Three-dimensional reconstitution of embryonic cardiomyocytes in a collagen matrix: a new heart model system, *FASEB J.*, 1997, **11**, 683-694.
6. W. H. Zimmermann, C. Fink, D. Kralisch, U. Remmers, J. Weil and T. Eschenhagen, Three-dimensional engineered heart tissue from neonatal rat cardiac myocytes, *Biotechnol. Bioeng.*, 2000, **68**, 106-114.
7. Y. Haraguchi, *et al.*, Fabrication of functional three-dimensional tissues by stacking cell sheets in vitro, *Nat. Protoc*, 2012, **7**, 850-858.
8. T. Kikuchi, T. Shimizu, M. Wada, M. Yamato and T. Okano, Automatic fabrication of 3-dimensional tissues using cell sheet manipulator technique, *Biomaterials*, 2014, **35**, 2428-2435.
9. Y. Sawa, *et al.*, Tissue engineered myoblast sheets improved cardiac function sufficiently to discontinue LVAS in a patient with DCM: Report of a case, *Surg. Today*, 2012, **42**, 181–184.

10. Y. Xiao, *et al.*, Microfabricated perfusable cardiac biowire: a platform that mimics native cardiac bundle, *Lab Chip*, 2014, **14**, 869-882.
11. C. Fink, S. Ergun, D. Kralisch, U. Remmers, J. Weil and T. Eschenhagen, Chronic stretch of engineered heart tissue induces hypertrophy and functional improvement, *FASEB J.*, 2000, **14**, 669-679.
12. W. H. Zimmermann, *et al.*, Engineered heart tissue grafts improve systolic and diastolic function in infarcted rat hearts, *Nat. Med.*, 2006, **12**, 452-458.
13. H. Anderson, J. Yanni, M. R. Boyett, N. J. Chandler and H. Dobrzynski, The anatomy of the cardiac conduction system, *Clin. Anat.*, 2009, **22**, 99-113.
14. G. D. Thomas, Neural control of the circulation, *Adv. T. Physiol. Educ.*, 2011, **35**, 28-32.
15. D. Neal, M. S. Sakar, L. S. Ong and H. H. Asada, Formation of elongated fascicle-inspired 3D tissues consisting of high-density, aligned cells using sacrificial outer molding, *Lab Chip*, 2014, **14**, 1907-1916.
16. K. Deisseroth, Optogenetics, *Nat. Methods*, 2011, **8**, 26-29.
17. Z. Jia, *et al.*, Stimulating cardiac muscle by light: cardiac optogenetics by cell delivery, *Circ. Arrhythm. Electrophysiol.*, 2011, **4**, 753-760.
18. D. Neal, M. S. Sakar, R. Bashir, V. Chan and H. H. Asada, Mechanical characterization and shape optimization of fascicle-like 3D skeletal muscle tissues contracted with electrical and optical stimuli, *Tissue Eng. Part A*, 2015, doi:10.1089/ten.TEA.2014.0317.
19. S. Hinds, W. Bian, R. G. Dennis and N. Bursac, The role of extracellular matrix composition in structure and function of bioengineered skeletal muscle, *Biomaterials*, 2011, **32**, 3575-3583.
20. H. P. Clamann, Motor unit recruitment and the gradation of muscle force, *Phys. Ther.*, 1993, **73**, 830-843.
21. W. R. Legant, A. Pathak, M. T. Yang, V. S. Deshpande, R. M. McMeeking and C. S. Chen, Microfabricated tissue gauges to measure and manipulate forces from 3D microtissues, *Proc. Nat. Acad. Sci.*, 2009, **106**, 10097-10102.
22. L. G. Griffith and M. A. Swartz, Capturing complex 3D tissue physiology in vitro, *Nat. Rev. Mol. Cell Biol.*, 2006, **7**, 211-224.
23. H. Vandenburgh, *et al.*, Automated drug screening with contractile muscle tissue engineered from dystrophic myoblasts, *FASEB J.*, 2009, **23**, 3325-3334.
24. T. Boudou, *et al.*, A microfabricated platform to measure and manipulate the mechanics of engineered cardiac microtissues, *Tissue Eng. Part A*, 2012, **18**, 910-919.
25. M. S. Sakar, *et al.*, Formation and optogenetic control of engineered 3D skeletal muscle bioactuators, *Lab Chip*, 2012, **12**, 4976-4985.
26. W. H. Zimmermann, *et al.* Tissue engineering of a differentiated cardiac muscle construct, *Circ. Res.*, 2002, **90**, 223-230.
27. W. Bian, B. Liau, N. Badie and N. Bursac, Mesoscopic hydrogel molding to control the 3D geometry of bioartificial muscle tissues, *Nat. Protoc.*, 2009, **4**, 1522-1534.
28. K. Nagamine, T. Kawashima, S. Sekine, Y. Ido, M. Kanzaki and M. Nishizawa, Spatiotemporally controlled contraction of micropatterned skeletal muscle cells on a hydrogel sheet, *Lab Chip*, 2011, **11**, 513-517.
29. V. Chan, R. Bashir and H. H. Asada, Utilization and control of bioactuators across multiple length scales, *Lab Chip*, 2014, **14**, 653-670.
30. C. Cvetkovic, *et al.*, Three-dimensionally printed biological machines powered by skeletal muscle, *Proc. Nat. Acad. Sci.*, 2014, **111**, 10125-10130.
31. V. Chan, K. Park, M. B. Collens, H. Kong, T. A. Saif and R. Bashir, Development of miniaturized walking biological machines, *Sci Rep*, 2012, **2**, 857.
32. A. W. Feinberg, *et al.*, Muscular thin films for building actuators and powering devices, *Science*, 2007, **317**, 1366-1370.
33. J. C. Nawroth, *et al.* A tissue-engineered jellyfish with biomimetic propulsion, *Nat. Biotech.*, 2012, **30**, 792-797.
34. J. Xi, J. J. Schmidt and C. D. Montemagno, Self-assembled microdevices driven by muscle, *Nat. Mater.*, 2005, **4**, 180-184.
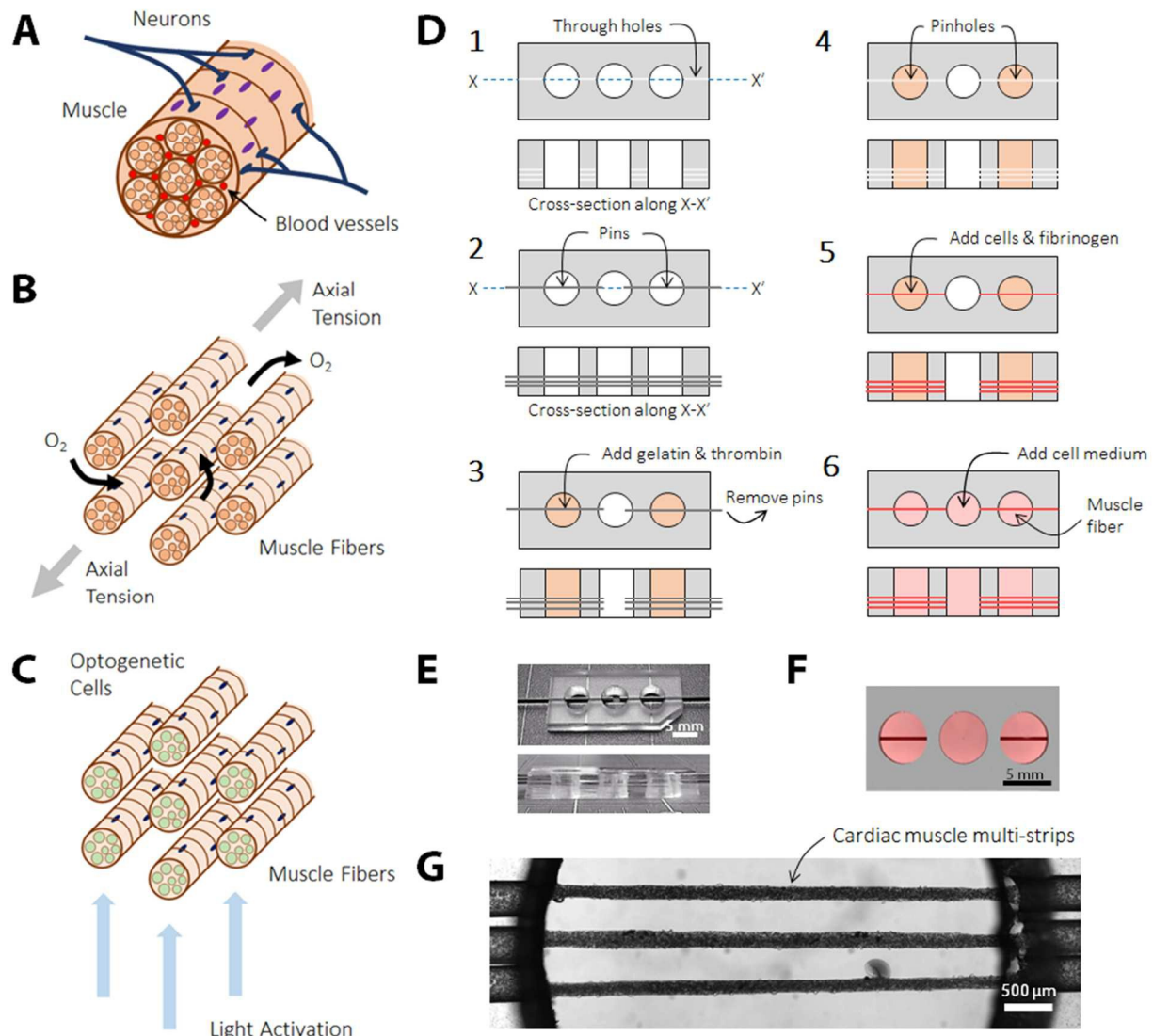
Fig. 1. Muscle tissue construct production technique utilizing sacrificial outer molding method and cell-mediated compaction. (A) Skeletal muscle fibers in vivo are supported by blood vessels and controlled by neurons. (B) Our in vitro construct spaces muscle strips evenly apart in an arrangement similar to skeletal muscle fibers in vivo to promote uniform perfusion of oxygen and nutrients. Both cardiac and skeletal muscle cells are capable of culture in this clustered fiber design. (C) Optogenetic technology was used to selectively recruit multiple muscle strips similar to in vivo muscle fiber control (D) Schematic overhead and cross-sectional view of multi-molding stage technique. Multiple pins can be utilized to produce clusters of individual muscle strips. (E) Photographic image of overhead and side view of PDMS platform with multiple pins. (F) Schematic image of PDMS platform with fully formed muscle strips. (G) Brightfield microscopy of multiple muscle strips by stitching together several acquired images.
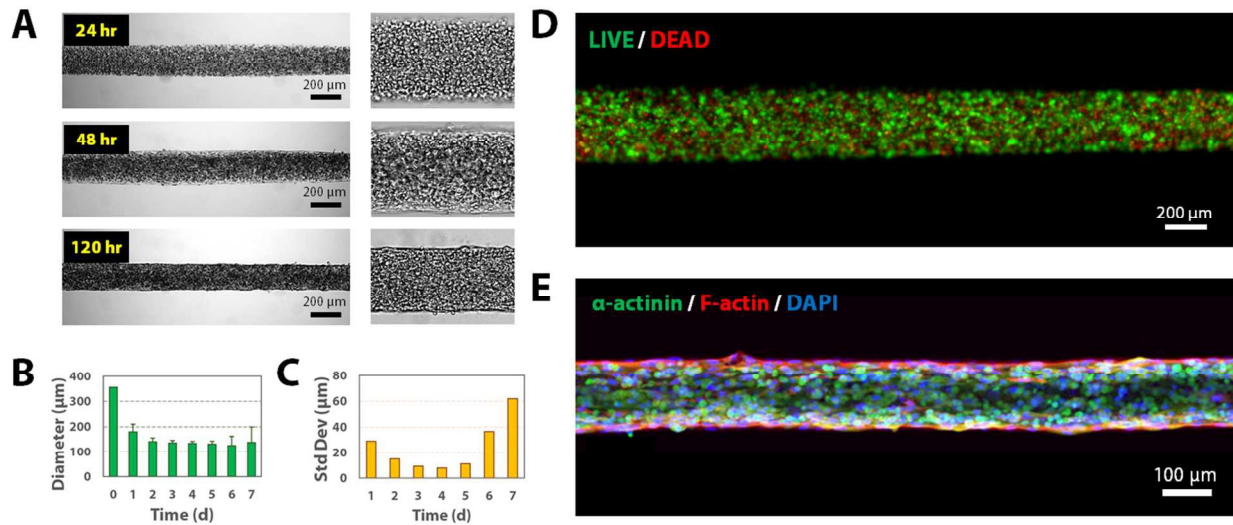
Fig. 2. Characterization of cardiac muscle tissue constructs. (A) Time-lapse brightfield microscopy of geometric changes in cardiac tissue construct. Images show high volumetric density of aligned cells, and anisotropic stress generated by cell-mediated compaction. (B) Mean diameters of individual muscle strips over time with 355 μm initial pin. (C) Standard deviation of individual muscle strips over time with 355 μm initial pin (indicative of strip degradation). (D) Viability of muscle tissue constructs evaluated with fluorescent-based calcein-AM/ethidium homodimer-1 assays after 6 hr. (E) Myocytes and fibroblasts incubated with fluorescently tagged with antibodies against mouse sarcomeric α-actinin, filamentous actin, and counterstained with DAPI (nuclei).
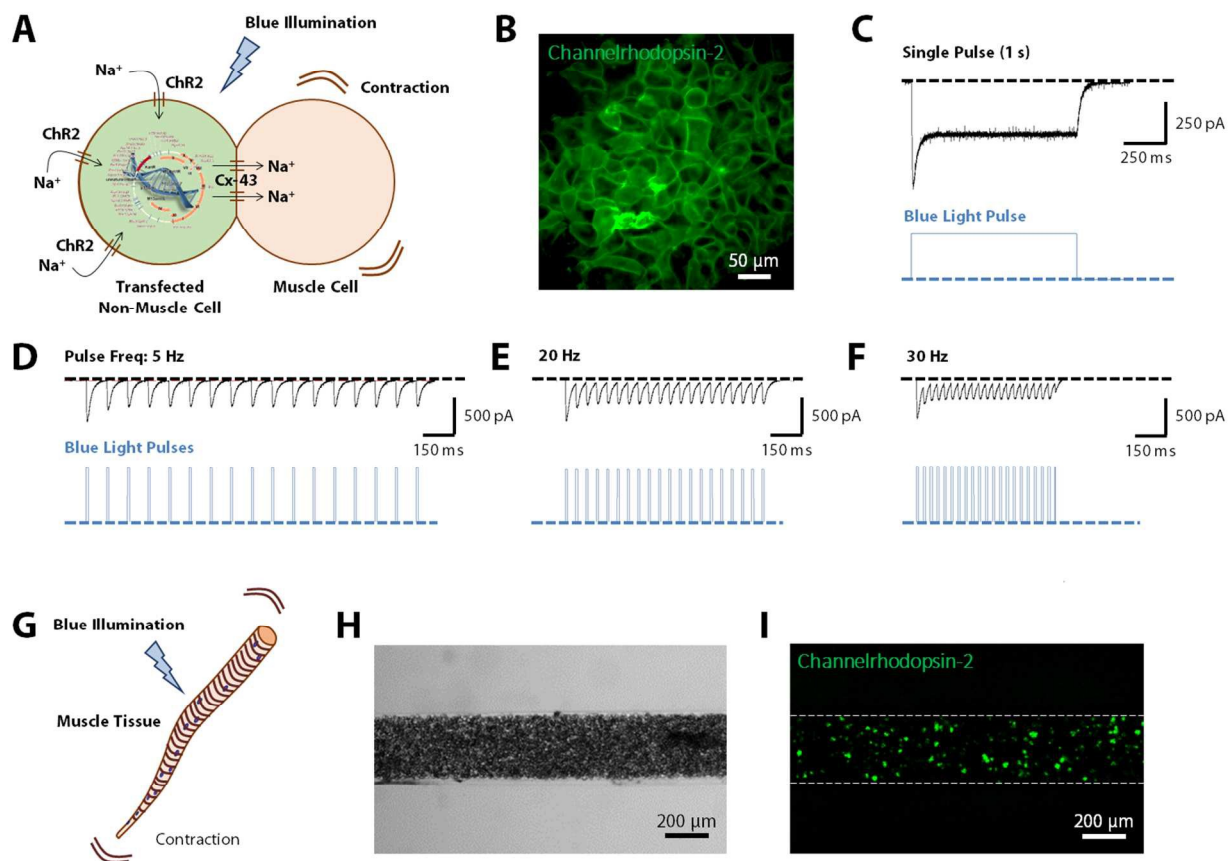
Fig. 3. Optogenetic manipulation of cardiac muscle via tandem cell unit strategy. (A) Utilization of nonexcitable HEK cells expressing channelrhodopsin-2 (ChR2) electrically coupled to myocytes to produce optically excitable heart tissue. (B) Stable HEK-ChR2 cell line shown with GFP-fluorescent reporter in the 10th passage after transfection and purification. Whole cell patch-clamping for quantification of the steady-state ChR2 current in single HEK–ChR2 cells at (C) single pulse, (D) 5 Hz, (E) 20 Hz, and (F) 30 Hz. (G) Schematic drawing for optical activation of cardiac muscle tissue constructs. (H) Brightfield microscopy of myocytes and HEK-ChR2 cells at 20:1 ratio in cardiac muscle tissue construct. (I) Fluorescent microscopy of HEK-ChR2 tagged with GFP-fluorescent reporter in cardiac muscle tissue construct.
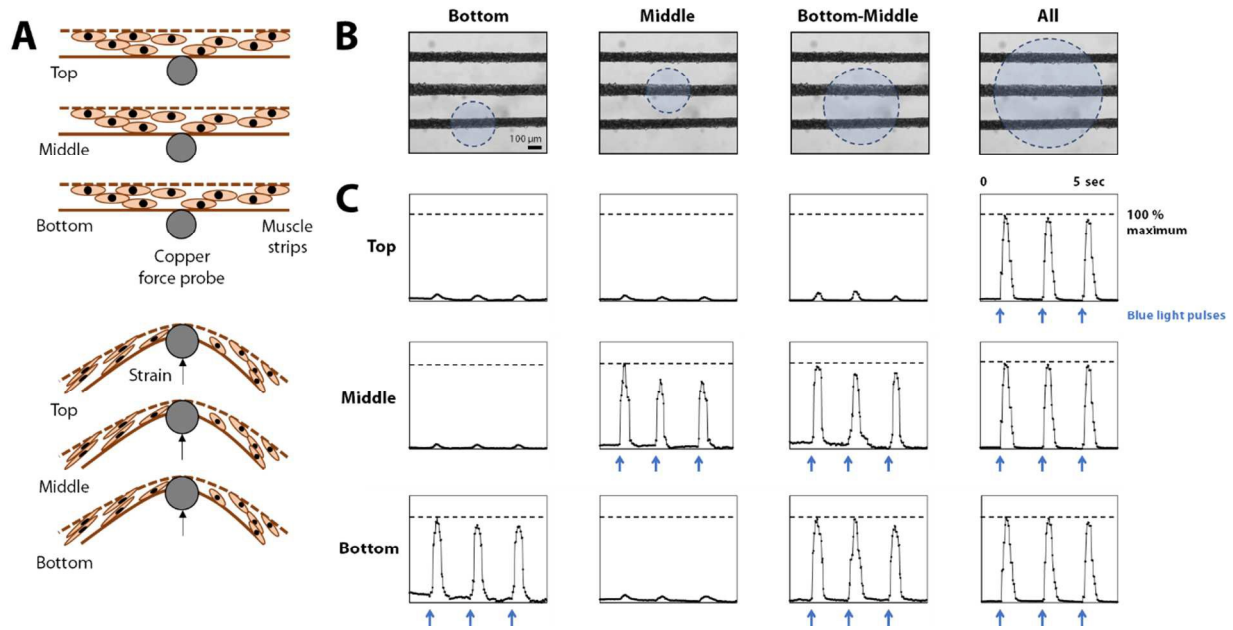
Fig. 4. Generation of light-induced stimulation and selective recruitment of optogenetic cardiac muscle tissue constructs. (A) Schematic drawing of optical setup for spatial control of blue light illumination. (B) Selective activation of cardiac muscle tissue constructs with local stimulation. Regions of exposure are labeled with blue transparent circles. (C) Verification that blue light pulses confined to a region stimulate only the cardiac muscle tissue constructs residing inside that specific region.
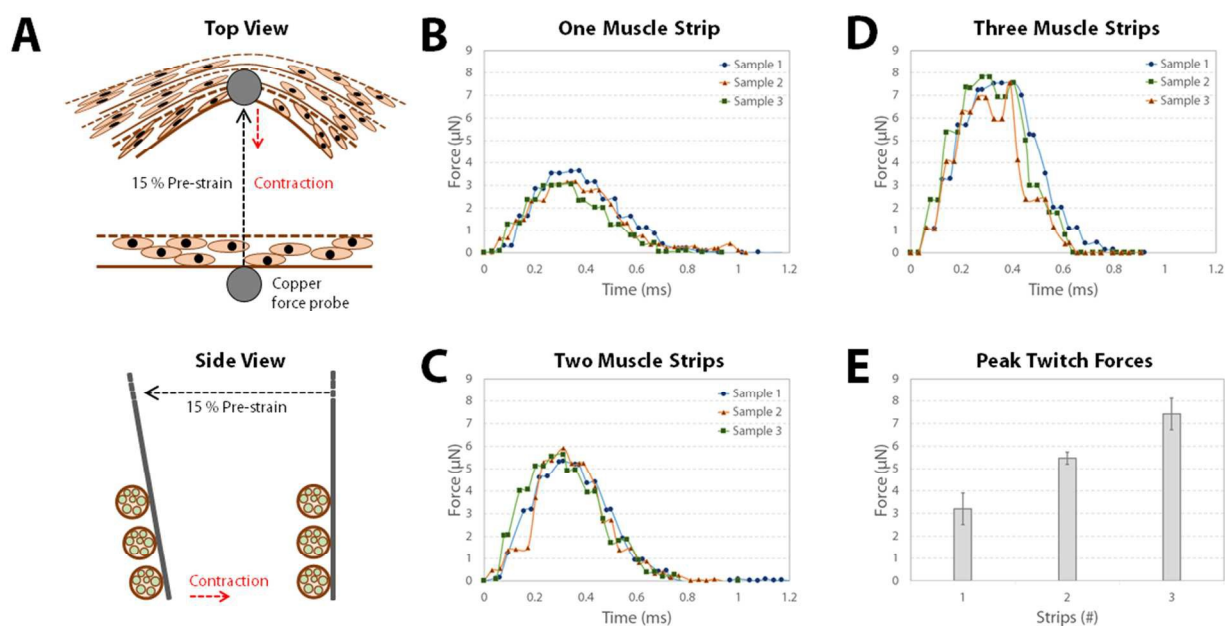
16

Fig. 5. Graded recruitment and force characterization of multi-strip muscles with micro force gauge. (A) A new micro force gauge was devised to characterize the cardiac muscle tissue construct properties. A copper probe with known stiffness was used to pull (B) one, (C) two, and (D) three muscle strips laterally a specified distance. Optical stimuli were then used to evaluate contractile performance. (E) The results indicate that force production of discrete numbers of recruited muscle strips is linear. The stiffness of the copper probe was k = 0.1487 N/m. The number of samples was n = 3, with six optically-induced twitches for each sample at 1 Hz.